

UNDERSTANDING SPINEL SPECTRA OF THE SINUS AESTUMM REGION USING MODIFIED GAUSSIAN MODEL. N. Chaudhuri¹, K.N. Kusuma¹ and S. A. Bharathvaj¹; ¹Department of Earth Sciences, Pondicherry University, Puducherry, India, 605014. (nabamitach93@gmail.com)

Introduction: One of the significant lunar pyroclastic deposits is found in the nearside Sinus Aestuum (SA) region of the moon [1][2]. But unlike the other major lunar pyroclastic deposits, the SA region is unusually water deficit [3]. It is also the only known location where Fe and Cr rich spinel is detected using orbiter datasets like Moon Mineralogy Mapper (M3) of Ch-1 and Spectral Profiler (SP) of Kaguya mission [4][5]. Various analysis of the M3 datasets has discovered Mg-Spinel as one of the dominant lithologies of the lunar surface. Surprisingly, spectral studies have shown the mineralogy of the spinel in the SA region is to be predominantly an Al-Fe rich pleonaste spinel and not Mg-rich [5]. Geomorphologically, the spinels of the SA region have a widespread distribution and are seen within fresh craters chiefly exposing extremely heterogenous highland materials [5]. We have attempted deconvolution on an M3 spectra of SA region to understand the nature of its constituent lithologies.

Datasets and Methodology: We have processed M3 reflectance datasets from the Chandrayaan-1 mission for deriving compositional information.

Integrated Band Depth (IBD). Absorption band positions and its corresponding band depth can be used to target mafic mineralogies of the lunar surface [5][6]. Based on the spectral absorption features of pyroxene and spinels, we have used the following IBD parameters:

$$\text{IBD at 700 nm} = \sum_{n=0}^{39} 1 - \frac{R(540 + 20n)}{R_c(540 + 20n)}$$

$$\text{IBD at 1000 nm} = \sum_{n=0}^{26} 1 - \frac{R(790 + 20n)}{R_c(790 + 20n)}$$

$$\text{IBD at 2000 nm} = \sum_{n=0}^{18} 1 - \frac{R(1658 + 40n)}{R_c(1658 + 20n)}$$

The color composite images were derived by assigning IBD1000, IBD2000 and IBD700 to red, green and blue channels respectively.

Modified Gaussian Model (MGM). Modified Gaussian model is a deconvolution technique which resolves overlapping absorption Gaussians into its corresponding individual end members [7][8]. The signal-to-noise ratio (SNR) of M3 is not adequate for deriving quantitative information from MGM derived Gaussian of its spectra but qualitative information can be deciphered [9].

Results: The spectra of Mg-spinel has a broad 2000 nm absorption without any 1000 nm absorption[10][11],

whereas Cr-spinel has a Visible-IR absorption feature at 700-750 nm and a 2000 nm absorption[4][12]. Thus, Cr-spinel will be indicated in the IBD color composite as cyan pixels. One such location in the SA region is the 'beacon' crater marked by Sunshine et al, 2014[13]. This area is identified with the strongest spinel absorption. When collected from various locations within the crater, the 700nm related absorption feature is seen in almost all spectra but its strength changes relative to the absorption feature of 1000nm. This shows the compositional heterogeneity of the region. Also, the non-identical band centers of the 1000nm reflectance minima indicate that the nature of the mafic mineral responsible for this absorption keeps differing within the crater. We have collected spectra averaged from the pixels of the crater for MGM deconvolution. The averaged spectra show visible-feature indicating the prominence of Cr-spinel in the region. The starting parameters were given keeping this spinel end member in mind. The end parameters deconvolve four gaussians at 4 different band centers, (i) 724 nm, (ii) 976 nm, (iii) 1913 nm, and (iv) 2201 nm. The first and the fourth band center identify with the absorption spectral features of a Cr-rich spinel. The 976 nm Gaussian is indicative of high-calcium pyroxene (HCP) whereas its corresponding 1913 nm Gaussian indicates low-calcium pyroxene.

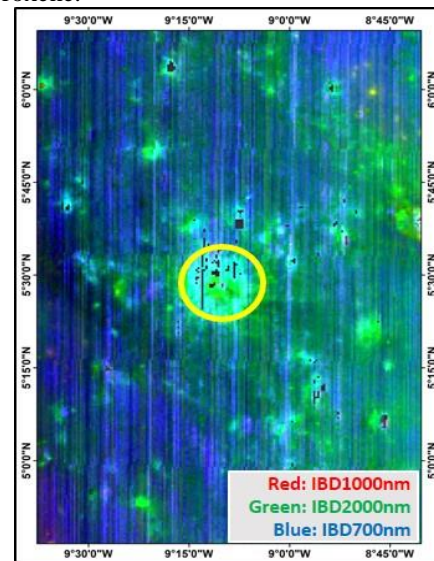


Figure 1: IBD color composite image derived from M3 image of the 'Beacon' crater (marked within the yellow circle) and its surrounding area. The bright cyan color indicates the presence of a strong visible and 2000 nm feature in the crater.

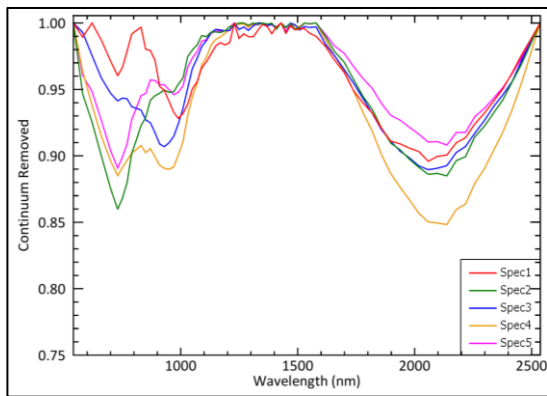


Figure 2: Continuum-removed spectra from various locations within the 'beacon' crater of figure 1.

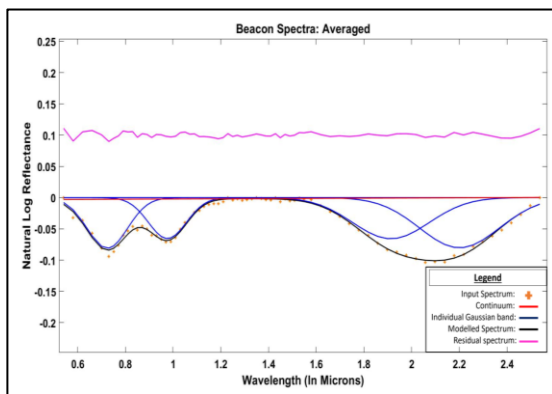


Figure 2: MGM derived gaussians for an M3 spectra averaged across the beacon crater.

Starting model parameters for MGM deconvolution for Averaged 'Beacon' crater spectra.

Band	Centre	FWHM	Strength
1	700±200	300±200	-0.03±200
2	1000±200	200±200	-0.08±100
3	1900±400	400±400	-0.03±400
4	2100±400	400±400	-0.03±400

Final model parameters for MGM deconvolution for Averaged 'Beacon' spectra.

Band	Centre	FWHM	Strength
1	724	199.74	-0.081
2	975.93	187.30	-0.066
3	1913.29	377.94	-0.066
4	2200.78	393.72	-0.080

Current RMS error = 3.908891e-03

Ongoing work: The low SNR of M3 makes finer deconvolution of the spectra unfeasible. The lack of proper corresponding gaussians for the HCP at longer wavelength and for LCP at shorter wavelength attests this limitation. We are currently working on the laboratory spectra of the Chromite and other mafic lunar analogue samples from Sittampundi Anorthosite Complex (SAC), India for better MGM-derived solutions. The higher spectral resolution of the laboratory spectra will help us to understand the spinel mineralogy better which can be extended to lunar samples.

References: [1] Gaddis, L.R. et al. (1985) *Icarus*, 61(3), 461-489. [2] Gaddis, L.R. et al. (2003) *Icarus*, 161, 262-280. [3] Milliken, R.E. and Li, S. (2017) *Nature Geoscience*, 10, 561-565. [4] Yamamoto, S. et al. (2013) *Geophysical Research Letters*, 40, 4549-4554. [5] Weitz, C.M. et al. (2017) *Journal of Geophysical Research: Planets*, 122, 2013-2033. [6] Besse, S. et al. (2011) *Journal of Geophysical Research*, 116(5), 1-15. [7] Sunshine, J.M. (1990) *Journal of Geophysical Research*, 93, 6955-6966. [8] Sunshine, J.M. and Pieters, C.M. (1993) *Journal of Geophysical Research*, 98, 9075-9087. [9] Isaacson, P.J. (2011) *Journal of Geophysical Research*, 119 [10] Pieters, C.M. et al (2011) *Journal of Geophysical Research*, 116(4), 1-14. [11] Dhingra, D. et al. (2011) *Geophysical Research Letters*, 38(11), 10-13. [12] Cloutis, E.A. et al. (2004) *Meteoritics and Planetary Science*, 39(4), 545-565. [13] Sunshine, J.M. et al. (2014) *LPSC 45th*, Abstract #2297